

OVERVIEW OF THE CERN PSB-TO-PS TRANSFER LINE OPTICS MATCHING STUDIES IN VIEW OF THE LHC INJECTORS UPGRADE PROJECT

V. Forte*, S. Albright, W. Bartmann, G. P. Di Giovanni, M. A. Fraser, C. Hessler, A. Huschauer, A. Oeftiger, CERN, Geneva, Switzerland

Abstract

At injection into the CERN Proton Synchrotron (PS) a significant horizontal emittance blow-up of the present high brightness beams for the LHC is observed. A partial contribution to this effect is suspected to be an important mismatch between the dispersion function in the transfer line from the PS Booster (PSB) and the ring itself. This mismatch will be unacceptable in view of the beam parameters requested by the LHC Injectors Upgrade (LIU) project with high longitudinal emittance and momentum spread. To deliver the requested beam parameters the PSB-to-PS transfer line will be upgraded and the optics in the line changed to improve the matching from all the four PSB rings. A re-matching campaign from the PSB ring 3 has been carried out to evaluate the impact of the present optics mismatch as a source of emittance growth both in simulations and measurements.

INTRODUCTION

The LIU project [1] at CERN aims at renovating the LHC injector chain in order to produce beams with twice the brightness. The achieved and future LIU beam parameters are reported in Table 1 [2]. The new high brightness LIU beams for the LHC foresee a higher longitudinal emittance ϵ_z and a larger contribution in momentum spread $\delta p/p_{rms}$ in order to keep the Laslett maximum transverse space charge tune shift ($\Delta Q_x, \Delta Q_y$) limited. The single bunch intensities N are doubled and the normalised horizontal (x) and vertical (y) transverse emittances ϵ will be similar to the values of today.

Table 1: LIU LHC Beam Parameters at PS Injection: Achieved and LIU Target [2]

Beam type	Energy [GeV]	N [$\times 10^{10}$ p]	ϵ_z [eVs]	$\epsilon_{x,y,0}$ [μm]	$\delta p/p_{rms}$ [$\times 10^{-3}$]	Tune spread [$\Delta Q_x, \Delta Q_y$]
Achieved						
LHC Standard	1.4	16.84	1.2	2.25	0.9	(0.25, 0.30)
LHC BCMS		8.05	0.9	1.2	0.8	(0.24, 0.31)
LIU						
LHC Standard	2	32.50	3	1.8	1.5	(0.18, 0.30)
LHC BCMS		16.25	1.48	1.43	1.1	(0.20, 0.31)

* vincenzo.forte@cern.ch

PRESENT PERFORMANCE OF LHC BEAMS AT PS INJECTION

An unexpected horizontal emittance growth in the order of $\sim 40\%$ is measured at PS injection during present operation. Figure 1 shows the statistics during LHC fills with BCMS bunches in 2018. The vertical emittance is preserved.

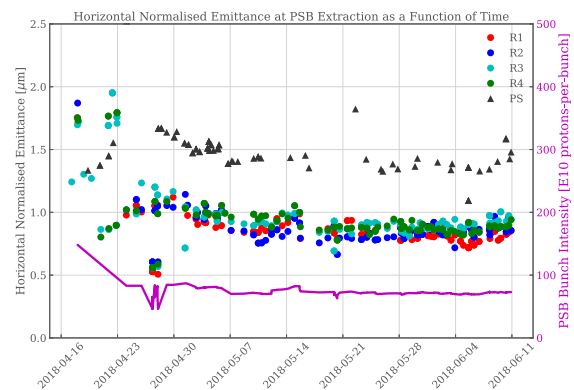


Figure 1: Horizontal emittances and intensity for LHC BCMS [3] beams at PSB extraction and PS injection during 2018 run.

To date, the beam injected into the PS has always been mismatched in dispersion with respect to the PS closed solution, as the simultaneous matching of the optics from the four rings of the PSB is not possible by using only ten available quadrupoles in the transfer line [4]. An eleventh quadrupole, which could improve the matching, would also be available but is placed inside a shielding wall and is not used in operation for safety and maintenance reasons. However, it is available for machine development (MD) purposes [5].

The LIU project imposes a budget of emittance growth of 5% between the PSB (extraction) and PS (extraction), thus the present dispersive mismatch would not be tolerated. In fact, by using the LIU parameters of Table 1 in the present optics, the horizontal dispersive mismatch would reach an unacceptable value of 30% at 1.4 GeV and 24% at 2 GeV (due to the difference in $\delta p/p_{rms}$). For this reason the transfer line between PSB and PS will be renovated after the Long Shutdown 2 (LS2) in 2020. In particular, the focusing structure in the transfer line between PSB and PS will be modified in order to provide dedicated optics settings for LIU [6]. Such optics will grant good matching in the horizontal plane, while some small residual and unavoi-

able mismatch is foreseen in the vertical plane due to edge focussing effects of the vertical recombination dipoles [7].

PSB-TO-PS TRANSFER LINE

The PSB-to-PS transfer line is composed of two parts: the first is the BT line, which is common with the other PSB users: in fact, by the means of a horizontal switching dipole, the bunches can be directed either to the PS (through the BTP line), or to the ISOLDE experiment [8], or to the PSB external beam dump, which is placed at the end of a measurement line (BTM). The BT line has five quadrupoles, which can be pulsed at every cycle with different values. The BTP line has six quadrupoles, including the one in the wall, whose values have to be kept constant for different cycles. Thus, only the five BT quadrupoles can be used in parallel operation for MD. However, they are not sufficient to guarantee a perfect analytical matching of eight parameters, i.e. Twiss ($\alpha_{x,y}$, $\beta_{x,y}$) and dispersion $D_{x,y}$ and $D'_{x,y}$.

Therefore, a re-matched optics which could minimise dispersion mismatch was computed using the MAD-X code [9] and used in MDs in 2017. The strengths of the quadrupoles that were used in 2017 parallel MDs are reported in Table 2.

Table 2: Operational and Re-matched (Dispersion-free) Optics for Parallel MDs: Normalised Quadrupolar Gradients k_1 and Currents I

Quadrupole	k_1 [m ⁻²]	I [A]	k_1 [m ⁻²]	I [A]
	Operational optics		Re-matched optics	
BT.QNO10	-0.66749	186	-0.92797	174.99
BT.QNO20	0.63160	176	0.66356	184.90
BT.QNO30	-0.28709	80	-0.26986	75.2
BT.QNO40	0.92347	256.79	0.99735	277.33
BT.QNO50	-0.73445	174.75	0.77117	183.49
BTP.QNO10	0	0	0	0
BTP.QNO20	0.52130	148.4	0.52130	148.4
BTP.QNO30	-0.48497	138.08	-0.48497	138.08
BTP.QNO40	0.62693	179.49	0.62693	179.49
BTP.QNO50	-0.53563	152.73	-0.53563	152.73
BTP.QNO60	0.6689	190.46	0.6689	190.46

SENSITIVITY ANALYSIS ON SINGLE QUADRUPOLE STRENGTH

A sensitivity analysis was performed by varying the BT.QNO10 strength, in order to optimise the mismatch factor $M_{\text{tot},x,y}$, as shown in simulation in Fig. 2, bottom-right. $M_{\text{tot},x,y}$ is defined as the quadratic sum of the components of emittance growth due to the betatron and dispersive mismatches, $M_{\beta_{x,y}}$ (Eq. (1) [10]) and $M_{D_{x,y}}$ (Eq. (2) [11]).

$$M_{\beta_{x,y}} = \frac{\Delta\epsilon_{x,y}}{\epsilon_{0,x,y}} = \frac{1}{2} \left[\frac{\beta_{x,y,\text{PS,closed}}}{\beta_{x,y,m}} + \frac{\beta_{x,y,m}}{\beta_{x,y,\text{PS,closed}}} + \left(\frac{\alpha_{x,y,m}}{\beta_{x,y,m}} - \frac{\alpha_{x,y,\text{PS,closed}}}{\beta_{x,y,\text{PS,closed}}} \right)^2 \beta_{x,y,\text{PS,closed}} \beta_{x,y,m} \right] - 1 \quad (1)$$

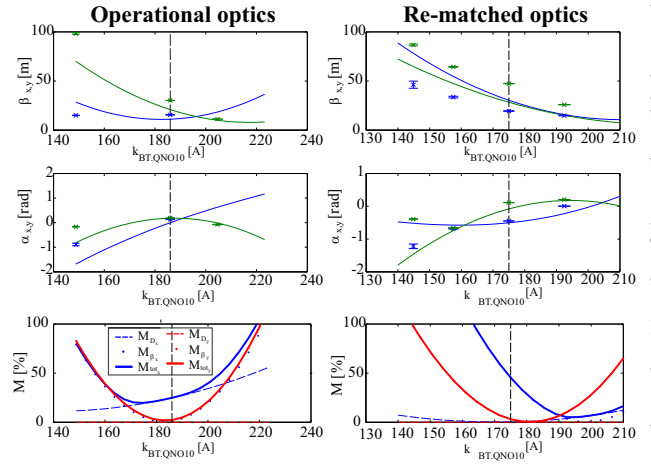


Figure 2: BT.QNO10 sensitivity analysis. Top-centre: simulated (solid lines) and estimated (markers with 1σ errorbar) $\alpha_{T,x,y}$ and $\beta_{T,x,y}$ from three screens measurements for the horizontal (blue) and vertical (green) planes. Bottom: simulated mismatch factors for $\epsilon_{0,x} = 1.1 \mu\text{m}$, $\epsilon_{0,y} = 1.05 \mu\text{m}$ and $\delta p/p_{\text{rms}} = 0.879 \times 10^{-3}$. The vertical dashed lines represent the nominal values.

$$M_{D_{x,y}} = \frac{\Delta\epsilon_{x,y}}{\epsilon_{0,x,y}} = \frac{1}{2} \frac{\Delta D_{x,y}^2 + (\beta_{x,y,T} D'_{x,y} + \alpha_{x,y,T})^2}{\beta_{x,y,T} \epsilon_{x,y,0,g}} \quad (2)$$

$$\left(\frac{\delta p}{p} \right)_{\text{rms}}^2 = \frac{1}{2} \frac{\Delta \bar{D}_{x,y}^2 + \Delta \bar{D}'_{x,y}^2}{\epsilon_{x,y,0,g}} \left(\frac{\delta p}{p} \right)_{\text{rms}}^2$$

where $\epsilon_{x,y,0,g}$ are the geometrical transverse emittances and $\beta_{x,y,m}$ and $\alpha_{x,y,m}$ are the Twiss parameters at the PS injection point (located at the end of the exit flange of septum in section 42), $\beta_{x,y,\text{PS,closed}}$ and $\alpha_{x,y,\text{PS,closed}}$ are the PS closed solutions, and $D_{x,y}$ and $D'_{x,y}$ are the components of the normalised dispersion vector, $\bar{D}_{x,y} = \frac{D_{x,y}}{\sqrt{\beta_{x,y}}}$ are the normalised dispersion components.

$\beta_{x,y,m}$ and $\alpha_{x,y,m}$ were estimated from a three-screen analysis [12] performed by measuring the single-pass beam profiles in three secondary emission monitor (SEM) grids placed just after injection in the PS. The analysis is based on the betatron beam sizes at the three grids. The betatron beam sizes are computed by quadratically subtracting the dispersive component from the total beam size measured at each grid, i.e.:

$$\sigma_{\beta_{x,y}} = \beta_{x,y} \epsilon_{x,y,g} = \beta_{x,y} \frac{\epsilon_{x,y}}{\beta_{\text{rel}} \gamma_{\text{rel}}} = \sqrt{\sigma_{\text{tot},x,y}^2 - D_{x,y}^2 \frac{\delta p^2}{p^2}}_{\text{rms}} \quad (3)$$

where β_{rel} and γ_{rel} are the relativistic Lorentz factors.

The results showed that the model and the measurements are in disagreement (see Fig. 2). Investigations are ongoing to understand the possible reasons, such as errors in the quadrupole transfer functions or the full deconvolution of the momentum distribution from the total beam [13].

Content from this work may be used under the terms of the CC BY 3.0 licence (© 2018). Any distribution of this work must maintain attribution to the author(s), title of the work, publisher, and DOI.

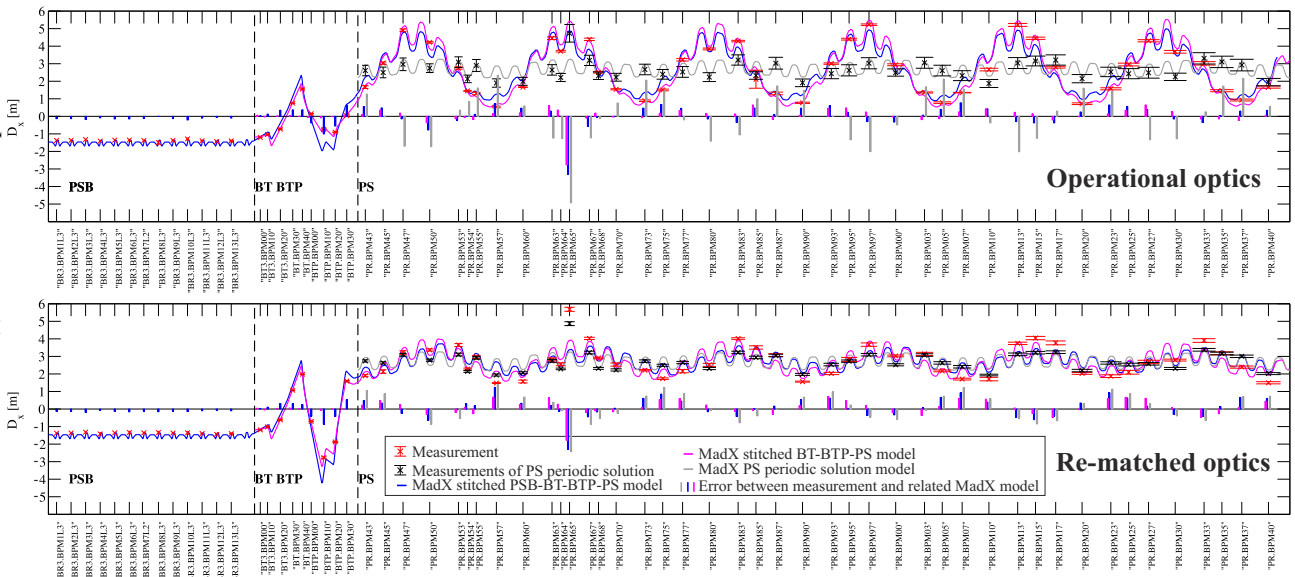


Figure 3: Dispersion measurements and simulations in the PSB-BT-BTP-PS line.

Nevertheless the analysis showed that the empirical $M_{\beta_{x,y}}$ is reduced to $\sim 3\%$ by increasing the current of BT.QNO10 by 10% in the re-matched optics. The three SEM grids are located in even numbered sections in the PS, where the closed solution of the Twiss parameters and dispersion functions are very similar. By correcting the current in BT.QNO10 by 10%, the total beam sizes measured at the location of the grids were very similar, indicating good matching. This optimisation is taken into account in the rest of the paper for the re-matched optics case. In order to confirm such a finding, a turn-by-turn beam profile matching monitor is, in this sense, fundamental; the fast electronics to make the SEM grid in section 52 able to read in multi-turn mode is in preparation and will be ready at the end of June 2018.

Transfer Line Initial Conditions

The initial conditions of the Twiss parameters at the beginning of the transfer line were measured using the three-screen method in the SEM grids of the BTM line with the operational optics, by using different beams. In particular, low intensity single LHC bunches with different of $\delta p/p_{rms}$ values were used in order to have a negligible influence of the dispersive profile contribution. Results showed good agreement with the nominal extraction parameters [14].

DISPERSION MEASUREMENTS

Dispersion measurements from the PSB to the PS were performed for both optics. The dispersion was measured by varying the extraction radio-frequency (RF) frequency, e.g. momentum, of the PSB and linearly correlating the related momentum offset to the positions recorded on beam position monitors (BPM) from the PSB (last turn) to the PS (first turn). The measurements showed a good correlation between model and measurements after re-matching the initial conditions of the dispersion model at the beginning of the BT line, as shown in Fig. 3. Dispersion in a drift behaves

like a ray. Hence the initial conditions of $D_{x,y}$ and $D'_{x,y}$ were calculated by linearly extrapolating to the beginning of the line the value of dispersions measured at the first two BPMs of the line which are placed in a drift region.

The dispersion was measured turn-by-turn in the PS. Measurements in Fig. 4 were performed by switching the RF cavities OFF. In fact, before the beam de-bunches inside the machine, it is possible to record the beam position for several turns from which one can derive the PS dispersion closed solution and the maximum amplitude of the normalised dispersion vector \bar{D} .

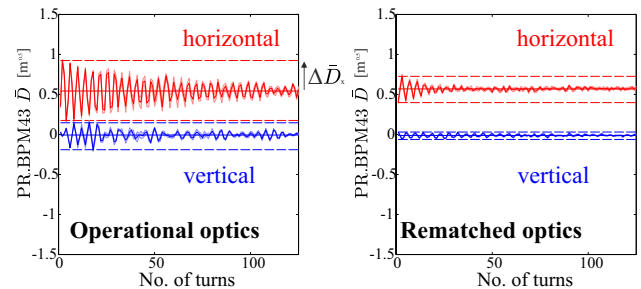


Figure 4: Turn-by-turn dispersion measurements in the PS around the closed solution (solid horizontal lines) keeping the RF cavities OFF at the first PS BPM after injection.

Dispersive Mismatch Factor $\lambda_{x,y}$ from Dispersion Measurements

The amplitude of the turn-by-turn dispersion oscillation around its closed solution was used to approximate the emittance growth due to dispersive mismatch of Eq. (2) to:

$$M_{D_{x,y}} \approx \lambda_{x,y} \frac{1}{\epsilon_{x,y,0,g}} \left(\frac{\delta p}{p} \right)_{rms}^2, \quad \lambda_{x,y} = \frac{1}{2} \max(\Delta \bar{D}_{x,y}^2) \quad (4)$$

The advantage of using this approximation is that the term $\lambda_{x,y}$ is a constant at every PS BPM and can be directly cal-

culated from measurements. In fact, $\max(\Delta\bar{D}_{x,y})$ represents the amplitude of the normalised dispersion mismatch vector when $\Delta\bar{D}'_{x,y} = 0$. Figure 5 shows the result of the calculation of $\lambda_{x,y}$ for the horizontal and vertical plane in the two considered optics. Figure 6 shows a color map of M_{D_x} for the operational optics (calculated $\lambda_{\text{average},x}=0.08$) by using Eq. (4).

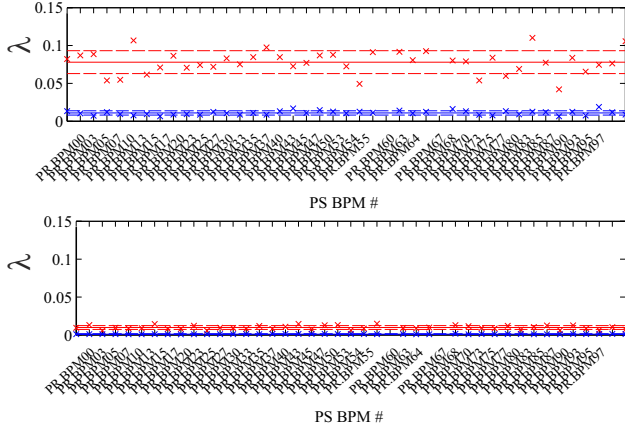


Figure 5: The $\lambda_{x,y}$ factor for the operational (top) and re-matched (bottom) optics in the horizontal (red) and vertical (blue) planes at the PS BPM locations. The horizontal solid lines represent the average value, the horizontal dashed lines are ± 1 standard deviation.

Thus, M_{D_x} for an operational BCMS beam, i.e. $\epsilon_{0,x,y} = 1 \mu\text{m}$ and $\delta p/p_{\text{rms}} = 0.9 \times 10^{-3}$, is $\sim 15\%$, while it is 8 times smaller (2%) in the case of re-matched optics, as $\lambda_{\text{average},x} = 0.01$ in this case. The estimated M_{D_y} is $< 2\%$ for such beams, thus negligible. Table 3 shows the summary for the two optics.

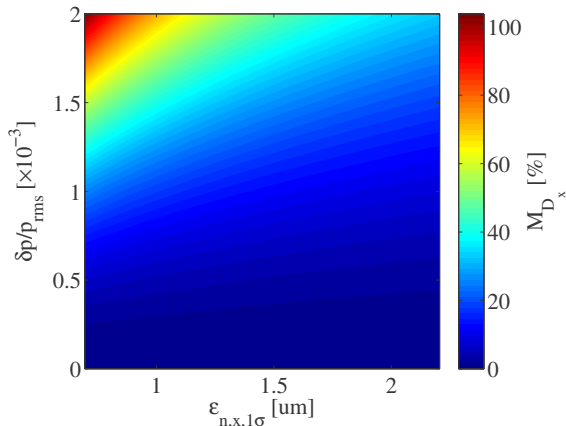


Figure 6: Operational optics: estimated emittance growth related to dispersion mismatch for different emittances and momentum spreads (see Eq. (4)) at 1.4 GeV.

Dispersive Mismatch Factor $\lambda_{x,y}$ from Emittance Measurements

If the dispersive effect is dominant in terms of emittance growth, it should be possible to derive the dispersive mis-

Table 3: Summary of expected emittance growth for operational and re-matched optics, derived from three-screen and dispersion measurements using Eqs. (1) and (4).

	$M_{\beta x}$ [%]	$M_{\beta y}$ [%]	M_{Dx} [%]	M_{Dy} [%]	$M_{\text{tot},x}$ [%]	$M_{\text{tot},y}$ [%]
Operational optics	6	6	15	2	16	6
Rematched optics	3	3	2	0	4	3

match factor $\lambda_{x,y}$ from transverse emittance blow-up $\Delta\epsilon_{x,y}$ measurements. In fact, starting from Eq. (4), one can derive

$$\lambda_{x,y} = \frac{\Delta\epsilon_{x,y}}{\beta_{\text{rel}}\gamma_{\text{rel}} \frac{\delta p^2}{p^2}_{\text{rms}}} \quad (5)$$

Measurements of LHC Standard “long” bunches, i.e. total bunch length of 210 ns, at different longitudinal emittances were performed in 2017 in the operational optics in order to assess the expected dependency of the blow-up with the momentum spread for large longitudinal emittance beams and also assess the threshold in which space charge might dominate. Figure 7 shows a clear linear correlation between emittance growth and $(\delta p/p_{\text{rms}})^2$ for longitudinal emittance larger than 1.6 eVs. For lower longitudinal emittances, other effects are dominant. Suspected cause could be the interaction with the horizontal PS integer resonance $Q_x = 6$ due to transverse space charge. For larger longitudinal emittances, the slope of the linear fit in the plot (divided by $\beta_{\text{rel}}\gamma_{\text{rel}}$) corresponds to the value of λ_x . However the calculated $\lambda_x \approx 0.3$ is much higher than the one derived from the previous dispersive measurements, suggesting again that other phenomena are involved in the emittance growth on top of the dispersive mismatch.

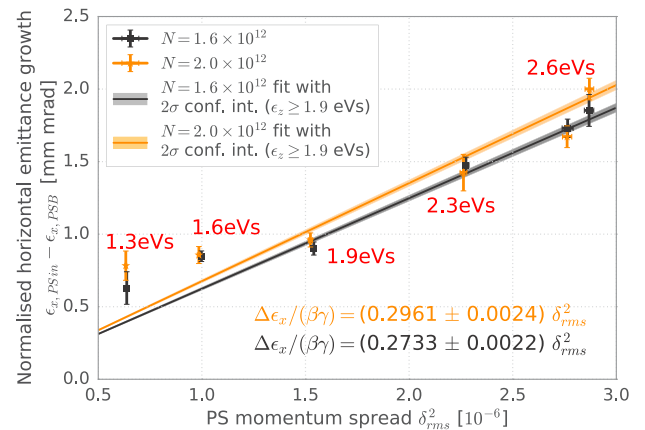


Figure 7: Correlation between normalised transverse emittance growth and energy spread squared for LHC Standard “long” bunches. Transverse emittances are calculated by deconvolving the non-Gaussian momentum spread distribution [13]. The slope remains the same for the usual Gaussian least-squares fit to determine the transverse emittance.

TRANSVERSE EMITTANCE MEASUREMENTS

The transverse emittance was measured during the sensitivity scan analysis for PSB R3 single BCMS bunches of $\sim 83 \times 10^{10}$ ppb. The cycle was set in order to have reduced coupling, low chromaticity and transfer feedback ON. The measurements are shown in Fig. 8. The emittance at extraction from the PSB was evaluated through the PSB wirescanner and three SEM grids in the BTM line. The two different techniques used to measure emittance give different results [15].

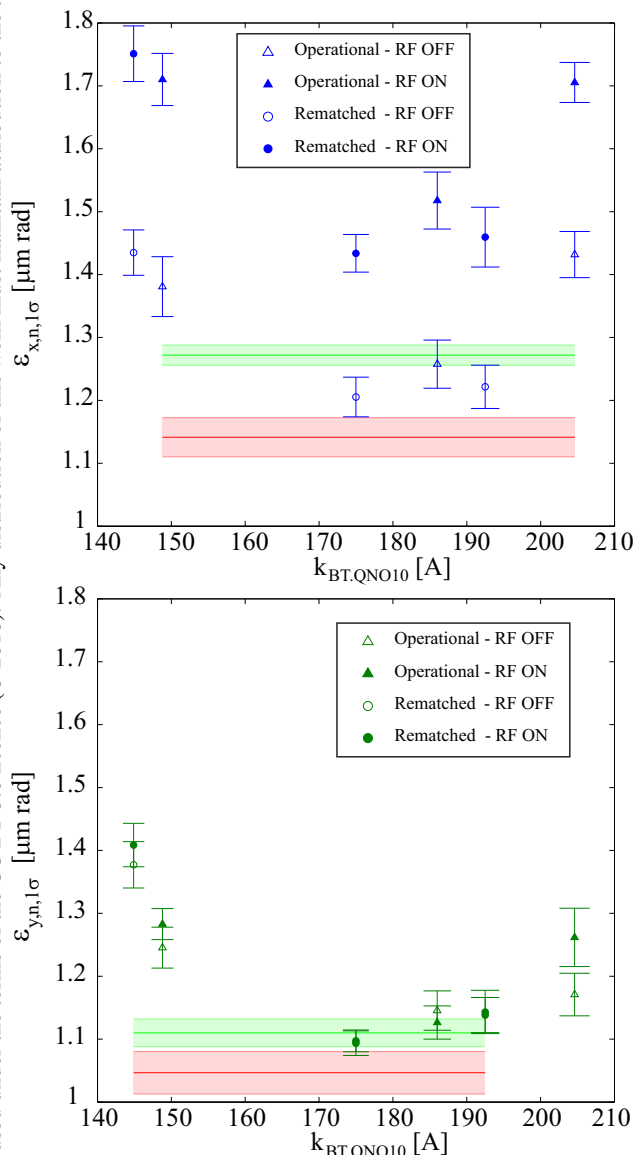


Figure 8: Normalised rms horizontal (top) and vertical (bottom) transverse emittances during the sensitivity scan of BT.QNO10. The horizontal errorbars are measurements performed with the PSB wirescanner (red) and the three SEM grids in the BTM line (green).

In the PS, the emittances are measured 15 ms after injection and are calculated from the Gaussian fit of the total

profile by using momentum spread subtraction in quadrature, as in Eq. (3). Only a slight reduction was achieved for the horizontal emittance. However, a big jump in the horizontal plane ($\sim 0.2\text{-}0.3 \mu\text{m}$) is present between the measurements done with the RF cavities ON or OFF. Investigations on the sources of such discrepancy are on-going.

CONCLUSIONS AND OUTLOOK

An unexpected horizontal emittance growth in the order of 40-50% is measured after injection in the machine for LHC beams. The PS operates with a large horizontal dispersion mismatch, which will be compensated for the future LIU optics. In order to assess whether such blow-up is related to optics mismatch between the PSB-to-PS transfer line and the PS, a thorough analysis of the transfer line optics from PSB to PS was performed in 2017. The measured horizontal mismatch for the operational optics is in the order of 16% for LHC BCMS beams and justifies only partially the measured emittance growth. The large dispersive mismatch was compensated by the means of a new optics, which can be used in parallel operation. A sensitivity scan of the gradient of a single quadrupole in the line allowed to optimise the matching, leading to an expected empirical total emittance growth induced by betatron and dispersive mismatches $<5\%$.

However, emittance measurements performed with the wirescanner showed only a slight improvement, but underlined a clear difference when the RF cavities in the PS are ON or OFF.

Further investigations are continuing in 2018, focussing on a new dedicated optics with full analytical matching to the PS, on the effect of the RF on the bunches at injection and on an improved knowledge of the present transfer line parameters, e.g. quadrupole gradients error through kick response analysis.

ACKNOWLEDGEMENTS

The authors would like to thank the PSB and PS operation teams for the constant support during the measurements.

REFERENCES

- [1] The LIU project: <https://espace.cern.ch/liu-project/default.aspx>
- [2] G. Rumolo, "LIU Target Beam Parameters", CERN EDMS: 1296306
- [3] H. Damerau *et al.*, "LHC Injectors Upgrade Technical Design Report", CERN-ACC-2014-0337
- [4] A. Jansson, M. Lindroos, M. Martini, and K. Schindl, "Study of emittance blowup sources between the PS booster and the 26-GeV PS", CERN-PS-98-058-OP
- [5] M. Benedikt *et al.*, "Study of a new PSB-to-PS transfer line optics with improved dispersion matching by means of turn-by-turn beam profile acquisitions", PS/AE/Note 2001-003 (MD)
- [6] W. Bartmann *et al.*, "New PSB H⁻ Injection and 2 GeV Transfer to the CERN PS", in *Proc. HB'14*, East-Lansing, MI, USA, paper WEO4AB02, pp.320.

- [7] W. Bartmann, V. Forte, and M. Fraser, “Emittance growth at PS injection according to model”, Presentation at CERN Machine Studies Working Group Meeting (MSWG), <https://indico.cern.ch/event/578789>
- [8] The ISOLDE experiment: <http://isolde.web.cern.ch/active-experiments>
- [9] MAD - Methodical Accelerator Design: <http://mad.web.cern.ch/mad/>
- [10] M. Giovannozzi, “Sources of emittance growth”, CERN Accelerator School (CAS) 2009.
- [11] B. Goddard *et al.*, “Expected emittance growth and beam tail repopulation from errors at injection into the LHC”, in *Proc. PAC’05*, Knoxville, TN, USA, 2005, paper MPPE011, pp. 1266.
- [12] G. Arduini *et al.*, “Measurement of the optical parameters of a transfer line using multi-profile analysis”, CERN-PS-98-032-CA
- [13] A. Oeftiger, H. Bartosik, A. Findlay, S. Hancock, and G. Rumolo, “Flat bunches with a hollow distribution for space charge mitigation”, in *Proc. IPAC’16*, Busan, Korea, pp. 652–655, doi:10.18429/JACoW-IPAC2016-MOPOR023
- [14] V. Forte, M. A. Fraser, and W. Bartmann, “Status of injection and transfer studies”, Presentation at LIU PS beam dynamics meeting, <https://indico.cern.ch/event/671971/>
- [15] G. P. Di Giovanni *et al.*, “Comparison of Different Transverse Emittance Measurement Techniques in the Proton Synchrotron Booster”, presented at IPAC2018, Vancouver, BC, Canada, paper MOPMF054.